



## Special Feature: Dynamics Modeling Supporting Vehicle Performance

Research Report

### Elastic Buckling Analysis for Compression and Torsion in Thin-walled Box Beams

Katsuya Furusu, Tatsuyuki Amago and Toshiaki Nakagawa

Report received on Jul. 4, 2016

**■ABSTRACT■** Recently, high-strength steel is being increasingly used in the plates that constitute the frames of vehicles. Since these plates are becoming thinner, the buckling is an important issue in the automotive industry. A variety of solutions to this problem have been proposed, some of which are currently in practical use. In this paper, an equation is first derived for simply expressing the shear stress on plates subjected to torsional buckling in the box beams that make up the frame. Although a precise equation can be derived using the energy method, this equation is complex and difficult to implement. Therefore, an approximation equation is proposed based on this precise equation and shear buckling stress of plates. The accuracy of the proposed equation is evaluated by comparing it to the results of an analysis using the finite element method (FEM). It is found that the difference in shear stress under torsional buckling is less than about 5% for a cross-sectional aspect ratio of 0.4-1.0. Then, an interaction formula for compressive and shear stresses is derived for thin-walled box beams subjected to a compressive force and torsional torque based on the well-known buckling stress interaction formulas for a plate. The accuracy of the proposed interaction formula is then evaluated by comparing with the results of FEM calculations. It is shown that the well-known equations for the plates can be obtained by approximating the buckling eigen equations derived using the energy method, assuming a deformed shape with low-order terms. In addition, the proposed interaction formula is found to be different depending on the structural parameters used.

**■KEYWORDS■** Buckling, Thin-walled Box Beam, FEM, Buckling Stress Interaction Formula, Torsion

#### 1. Introduction

In the initial design of vehicle bodies, the full plastic strength of the frame section is typically evaluated to determine the sectional shape, accounting for static strength, rigidity, and collision performance. Basing the evaluation on the full plastic strength effectively utilizes all the steel plating comprising the cross section, and the strength is determined with all the sheet plates at their yield point.

In modern vehicle bodies, the use of high-strength steel plates is becoming increasingly common in order to reduce weight while maintaining strength, and this is resulting in progressively thinner frame structures. When external forces act upon such thin-walled frames, their rigidity sometimes decreases before plastic deformation occurs. This is mainly because, as the thin plates elastically buckle under compressive stress, areas of the section lose their ability to spread the load. The thinner the plates, the more susceptible they are to elastic buckling. Since buckling also reduces

the maximum load before plastic collapse, evaluations based on the full plastic strength may overestimate the strength. Thus, various evaluation methods have been proposed and are currently in practical use to replace those using the full plastic strength. Effective width theory is one method of analyzing the effects of elastic buckling, and strength evaluations have been proposed based on this theory. Using computer-aided engineering (CAE), an application of the finite element method (FEM), rigidity and strength can be calculated to a high degree of accuracy.

However, building a CAE calculation model in the initial stages of design is difficult since the vehicle shape is often not completely fixed. Also, it is not easy to redesign the basic shape, even if it turns out that it will not meet the design requirements after the detailed shape is fixed. Therefore, it is important to understand elastic buckling phenomenon for thin-walled frames at the initial design stages in order to create an effective design and develop vehicle frames efficiently.

Buckling of thin-walled frames is analyzed based on

buckling of the constituent plates, and there have been several past studies on plate buckling.<sup>(1-5)</sup> For flexural and shear buckling, solutions can be accurately approximated using the energy method,<sup>(6,7)</sup> with an infinite sinusoidal series representing the buckling deformed shape. Further, both the buckling stress and post-buckling behavior of a thin-walled structure must be known in order to determine its yield strength, and effective width theory for elastic buckling is one approach to determining these factors.<sup>(8,9)</sup> Commercially available software<sup>(10)</sup> exists that has analysis functions based on this theory, and methods for estimating the strength that account for elastic buckling have been proposed. For simply supported square plates that in-plane displacements of the surrounding edges are constrained as straight lines, using a stress function that applies the energy method to a formula describing large deflections of plates,<sup>(11)</sup> there are methods<sup>(5,12)</sup> for determining the compressive post-buckling stress distribution and the load displacement relationship, without directly using effective width theory. Body frame members can be regarded as beams with rectangular cross sections (hereinafter “box beams”), and the basic loads acting upon the frame are an axial compressive force, a torsional torque, and a bending moment, or some combination thereof. In terms of buckling of box beams, the buckling stress for the axial compressive force has been solved.<sup>(13-16)</sup> For square sections, the interaction formula have been determined for combinations of compression and torsion, and bending and torsion.<sup>(17,18)</sup>

In this report, we present a method for determining elastic buckling for basic loads acting upon the box beam illustrated in **Fig. 1**,<sup>(19)</sup> particularly for the case of a compressive force, a torsional torque, and a combination of the two. First, equations are derived for approximating the shear buckling stress when a torsional torque ( $T$ ) acts on a box beam. Next, after considering the buckling stress interaction formula for plates under combined loads (**Fig. 2**),<sup>(20)</sup> we propose an interaction formula relating compressive and shear buckling stresses when an axial compressive force and a torsional torque act together upon the box beam.

The FEM is often used to investigate various performances of vehicle structures, including structural rigidity and yield strength, as well as crash safety. Consequently, in this report, the results of FEM computations are taken as being correct and are used to

verify the accuracy of the derived equations. Also, since vehicle body frames are being considered, the aspect ratio (short side  $h$  / long side  $b$ ) for the box section is taken to be within the range 0.4-1.0. Similarly, the discussion applies to beams with rectangular plates with aspect ratios (width  $b$  or  $h$  / length  $l$ ) of 1/3 or lower.

## 2. Well-known Basic Equations for Buckling of Plate and Box Beam

Since the box beam studied in this report (**Fig. 1**) is made up of thin plates, in order to consider its buckling behavior, it is first necessary to review current research results for thin-plate buckling. This section will summarize existing research on buckling of rectangular plates due to compression, shearing, bending, or a combination of these forces. It will also describe research results for box beams.

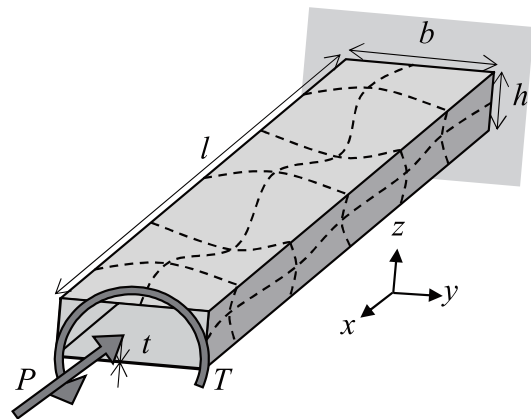


**Fig. 1** Schematic view of box beam subjected to compressive force and torsional torque.

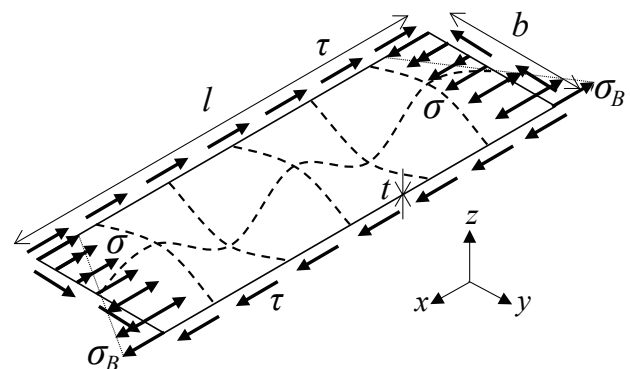


**Fig. 2** Schematic view of rectangular plate under combined loads.

## 2.1 Buckling of Rectangular Plates and Buckling Stress Interaction Formula

We will consider a simply supported rectangular plate with a length  $l$ , width  $b$ , and thickness  $t$  as shown in Fig. 2 (Young's modulus is  $E$  and Poisson's ratio is  $\mu$ ). As shown in the figure, when a compressive stress  $\sigma$ , shear stress  $\tau$ , and bending stress  $\sigma_B$  independently act upon the rectangular plate, the buckling stresses  $\hat{\sigma}_{cr}$ ,  $\hat{\tau}_{cr}$ , and  $\hat{\sigma}_{Bcr}$  are as given by<sup>(1,2,4)</sup>

$$\hat{\sigma}_{cr} = k_C \sigma_e, \quad k_C = 4.00, \quad (1)$$

$$\sigma_e = \frac{\pi^2 E}{12(1-\mu^2)} \left(\frac{t}{b}\right)^2, \quad (2)$$

$$\hat{\tau}_{cr} = k_S \sigma_e, \quad k_S = 5.34 + 4.00 \left(\frac{b}{l}\right)^2, \quad (3)$$

$$\hat{\sigma}_{Bcr} = k_B \sigma_e, \quad k_B = 23.9. \quad (4)$$

Note that the buckling stresses for an individual plate are written with a carat (^) to differentiate them from the buckling stresses for the box beam. For buckling under combined loads, the acting stresses are expressed using a buckling stress interaction formula. For compression, shearing, and flexural buckling, with stress components of  $\hat{\sigma}'_{cr}$ ,  $\hat{\tau}'_{cr}$ , and  $\hat{\sigma}'_{Bcr}$ , respectively, compression and shearing are related as:

$$\frac{\hat{\sigma}'_{cr}}{\hat{\sigma}_{cr}} + \left(\frac{\hat{\tau}'_{cr}}{\hat{\tau}_{cr}}\right)^2 = 1, \quad (5)$$

$$\left(\frac{\hat{\sigma}'_{Bcr}}{\hat{\sigma}_{Bcr}}\right)^2 + \left(\frac{\hat{\tau}'_{cr}}{\hat{\tau}_{cr}}\right)^2 = 1, \quad (6)$$

$$\frac{\hat{\sigma}'_{cr}}{\hat{\sigma}_{cr}} + \left(\frac{\hat{\sigma}'_{Bcr}}{\hat{\sigma}_{Bcr}}\right)^2 + \left(\frac{\hat{\tau}'_{cr}}{\hat{\tau}_{cr}}\right)^2 = 1. \quad (7)$$

Equation (5) represents the buckling stress relationship determined by Iguchi,<sup>(21,22)</sup> expressed as a regression formula. Equation (6), presented by Chwalla,<sup>(23)</sup> is proposed as a regression formula that closely matches the theoretical analysis results. Equation (7) is based on the results of Johnson and Buchert,<sup>(24)</sup> and formulated as an equation by Ziemian et al.<sup>(4)</sup>

## 2.2 Box Beam Compression and Torsional Buckling

Kuranishi<sup>(13-16)</sup> investigated axial compression buckling for shearing of a box beam. He determined the buckling stress assuming no deflection in the ridge connecting two plates (maintaining a straight line), a ridge with no simple rotation support for the plates, a certain rigidity, and coupling between the deflection angle and the moment of the adjoining plates. The steps given here can be applied to any sectional shape formed by a combination of thin plates, not just rectangular sections. The buckling stress is expressed as:

$$\sigma_{cr} = k_C \sigma_e, \quad (8)$$

where  $k_C$  is the buckling stress coefficient, which is a function of the sectional aspect ratio ( $h/b$ ). As illustrated in Fig. 3,<sup>(20)</sup> this equation does have an explicit form.

Wittrick and Curzon<sup>(17,18)</sup> determined a buckling and buckling stress interaction formula for beams of infinitely long equilateral triangular and square sections under compression and torsion. It should be noted that the buckling deformation mode will vary greatly with load ratio and illustrates the relationship with buckling stress. Figure 4<sup>(20)</sup> depicts the buckling stress interaction formula curve in square box beams as determined by Wittrick and Curzon.

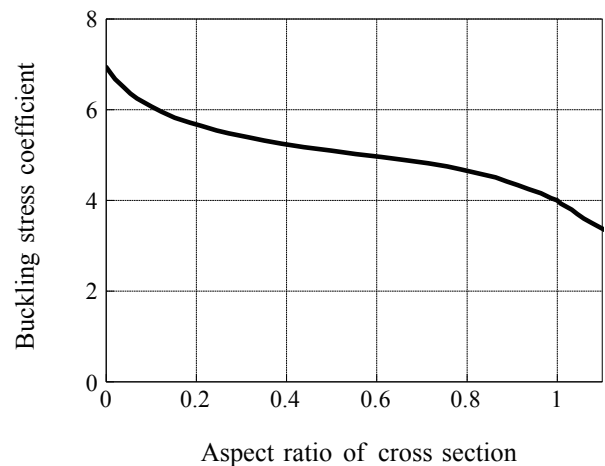


Fig. 3 Buckling stress coefficient vs. aspect ratio for cross section of box beam under compression.<sup>(13,20)</sup>

### 3. Shear Buckling Stress under Torsion by Energy Method

When torsional torque acts on a body frame, it can be thought of as a shear stress acting upon the plates comprising that section. The shear buckling stress on a single plate can be determined in simplified form, but there are few studies discussing the torsional buckling for box beams, as already mentioned in Sec. 2, and there is no equation to simply express the shear buckling stress under torsion. Wittrick and Curzon introduced the buckling stress interaction formula above, for when a torsional torque and an axial compression force act upon infinitely long rectangular box beams, and also mentioned the buckling stress in the case of torsional torque acting alone. However, the interaction formula by Wittrick and Curzon cannot be applied as it stands to rectangular sections with an arbitrary aspect ratio and a finite length. Thus, the objective in this section is to derive an equation to approximate the shear buckling stress and the buckling torque when a box beam is under torsion.

#### 3.1 Basic Formulae for Torsional Buckling of Box Beams

We will consider the box beam depicted in Fig. 1, comprising plates of width  $b$  (horizontal plates) and height  $h$  (vertical plates), assuming  $b \geq h$ , and a length  $l$  and thickness  $t$  (Young's modulus is  $E$  and Poisson's ratio is  $\mu$ ). When a torsional torque  $T$  acts upon one end of the beam, the relationship between  $T$  and the

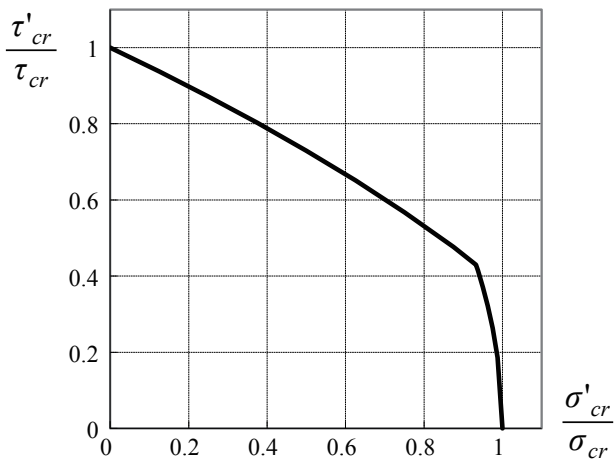


Fig. 4 Buckling stress interaction formula curve for square box beam under compression and torsion.<sup>(18,20)</sup>

plate shear stress  $\tau$  is given by:

$$T = 2bht\tau. \quad (9)$$

Taking the four plates as individual rectangular plates, the wider horizontal plates will buckle. Using Euler's buckling stress  $\sigma_e$  and the shear buckling coefficient  $k_s$ , the shear buckling stress  $\tau_{bc}$  is calculated as follows:

$$\tau_{bc} = k_s \sigma_e, \quad (10)$$

$$k_s = 5.34 + 4.00 \left( \frac{b}{l} \right)^2. \quad (11)$$

However, if shear buckling in the horizontal plates results in any out-of-plane deformation, this will also cause out-of-plane deformation in the vertical plates. Equation (10) only describes buckling in the horizontal plates in Fig. 1, and since it completely ignores the effects on the vertical plates, it is not suitable for directly determining the shear stress under torsional buckling.

#### 3.2 Shear Stress under Torsional Buckling Using the Energy Method

In this section, the shear buckling stress is determined for the box beam in Fig. 1 using the energy method, taking the out-of-plane displacement for the horizontal plates (z-axis direction) as  $w$ , and for the vertical plates (y-axis direction) as  $v$ . If both the horizontal and vertical plates are taken as being simply supported rectangular plates, their out-of-plane displacements under buckling can be expressed as:

$$w = \sum_{m=1}^{\infty} \sum_{n=1}^{\infty} B_{mn} \sin \frac{m\pi x}{l} \sin \frac{n\pi y}{b},$$

$$v = \sum_{m=1}^{\infty} \sum_{n=1}^{\infty} H_{mn} \sin \frac{m\pi x}{l} \sin \frac{n\pi z}{h}. \quad (12)$$

The plate inclinations at the shared edge of the horizontal and vertical plates are:

$$\left. \frac{\partial w}{\partial y} \right|_{y=0} = \sum_{m=1}^{\infty} \sum_{n=1}^{\infty} \frac{n\pi}{b} B_{mn} \sin \frac{m\pi x}{l},$$

$$\left. \frac{\partial v}{\partial z} \right|_{z=0} = \sum_{m=1}^{\infty} \sum_{n=1}^{\infty} \frac{n\pi}{h} H_{mn} \sin \frac{m\pi x}{l}. \quad (13)$$

If the out-of-plane displacement of the horizontal and

vertical plates are coupled, and the angles at their edges are assumed not to change after deformation, the coefficients  $B_{mn}$  and  $H_{mn}$  can be expressed using the shared coefficient  $\Phi_{mn}$  from Eq. (13) as:

$$\frac{B_{mn}}{b} = \frac{H_{mn}}{h} = \frac{\Phi_{mn}}{\sqrt{bh}}. \quad (14)$$

Using this equation,  $w$  and  $v$  can be expressed as:

$$w = \sum_{m=1}^{\infty} \sum_{n=1}^{\infty} \sqrt{\frac{b}{h}} \Phi_{mn} \sin \frac{m\pi x}{l} \sin \frac{n\pi y}{b},$$

$$v = \sum_{m=1}^{\infty} \sum_{n=1}^{\infty} \sqrt{\frac{h}{b}} \Phi_{mn} \sin \frac{m\pi x}{l} \sin \frac{n\pi z}{h}. \quad (15)$$

Thus, the strain energy  $U$  and the work  $W_s$  by the torsional torque for the four plates comprising the box beam can be expressed using  $w$  and  $v$  as:

$$U = 2 \times \frac{D}{2} \int_0^b \int_0^l \left\{ \left( \frac{\partial^2 w}{\partial x^2} + \frac{\partial^2 w}{\partial y^2} \right)^2 - 2(1-\mu) \left[ \frac{\partial^2 w}{\partial x^2} \frac{\partial^2 w}{\partial y^2} - \left( \frac{\partial^2 w}{\partial x \partial y} \right)^2 \right] \right\} dx dy$$

$$+ 2 \times \frac{D}{2} \int_0^h \int_0^l \left\{ \left( \frac{\partial^2 v}{\partial x^2} + \frac{\partial^2 v}{\partial z^2} \right)^2 - 2(1-\mu) \left[ \frac{\partial^2 v}{\partial x^2} \frac{\partial^2 v}{\partial z^2} - \left( \frac{\partial^2 v}{\partial x \partial z} \right)^2 \right] \right\} dx dz, \quad (16)$$

$$W_s = -2 \times t \int_0^b \int_0^l \tau \left( \frac{\partial w}{\partial x} \frac{\partial w}{\partial y} \right) dx dy - 2 \times t \int_0^h \int_0^l \tau \left( \frac{\partial v}{\partial x} \frac{\partial v}{\partial z} \right) dx dz, \quad (17)$$

$$D = \frac{Et^3}{12(1-\mu^2)}, \quad (18)$$

where  $\tau$  is the shear stress as calculated by Eq. (9), give the energy stationary condition of:

$$\frac{\partial}{\partial \Phi_{mn}} (U - W_s) = 0. \quad (19)$$

Calculating the definite integrals in Eqs. (16) and (17), solving for  $U$  and  $W_s$  for the four plates, and combining with Eq. (19) gives us the following:

$$\frac{\pi^2 \sigma_g l l}{32 \tau b h} \left\{ \left( \frac{b}{l} \right)^3 \left[ m^2 + \left( \frac{l}{b} \right)^2 n^2 \right]^2 + \left( \frac{h}{l} \right)^3 \left[ m^2 + \left( \frac{l}{h} \right)^2 n^2 \right]^2 \right\} \Phi_{mn}$$

$$- mn \frac{b h}{l l} \left[ \left( \frac{l}{b} \right)^2 + \left( \frac{l}{h} \right)^2 \right] \sum_i \sum_j \frac{ij \Phi_{ij}}{(i^2 - m^2)(j^2 - n^2)} = 0, \quad (20)$$

$$\sigma_g = \frac{\pi^2 E}{12(1-\mu^2)} \left( \frac{t}{l} \right)^2, \quad (21)$$

where the summation signs for  $i$  and  $j$  in Eq. (20) mean that they are only added when  $m+i$  and  $n+j$  are odd numbers. The matrix for Eq. (20) is:

$$\begin{bmatrix} \frac{\sigma_g}{\tau} \beta_0 \beta_2 & -\frac{4}{9} \beta_1 & 0 & 0 & 0 & \dots \\ -\frac{4}{9} \beta_1 & 16 \frac{\sigma_g}{\tau} \beta_0 \beta_2 & \frac{4}{5} \beta_1 & \frac{4}{5} \beta_1 & -\frac{36}{25} \beta_1 & \dots \\ 0 & \frac{4}{5} \beta_1 & \frac{\sigma_g}{\tau} \beta_0 \beta_3 & 0 & 0 & \dots \\ 0 & \frac{4}{5} \beta_1 & 0 & \frac{\sigma_g}{\tau} \beta_0 \beta_4 & 0 & \dots \\ 0 & -\frac{36}{25} \beta_1 & 0 & 0 & 81 \frac{\sigma_g}{\tau} \beta_0 \beta_2 & \dots \\ \vdots & \vdots & \vdots & \vdots & \vdots & \ddots \end{bmatrix} \begin{Bmatrix} \Phi_{11} \\ \Phi_{22} \\ \Phi_{13} \\ \Phi_{31} \\ \Phi_{33} \\ \vdots \end{Bmatrix} = \{0\}. \quad (22)$$

The constants here are:

$$\beta_0 = \frac{\pi^2 l l}{32 b h}, \quad (23)$$

$$\beta_1 = \frac{b h}{l l} \left\{ \left( \frac{l}{b} \right)^2 + \left( \frac{l}{h} \right)^2 \right\}, \quad (24)$$

$$\beta_2 = \left( \frac{b}{l} \right)^3 \left\{ 1 + \left( \frac{l}{b} \right)^2 \right\}^2 + \left( \frac{h}{l} \right)^3 \left\{ 1 + \left( \frac{l}{h} \right)^2 \right\}^2, \quad (25)$$

$$\beta_3 = \left( \frac{b}{l} \right)^3 \left\{ 1 + 9 \left( \frac{l}{b} \right)^2 \right\}^2 + \left( \frac{h}{l} \right)^3 \left\{ 1 + 9 \left( \frac{l}{h} \right)^2 \right\}^2, \quad (26)$$

$$\beta_4 = \left( \frac{b}{l} \right)^3 \left\{ 9 + \left( \frac{l}{b} \right)^2 \right\}^2 + \left( \frac{h}{l} \right)^3 \left\{ 9 + \left( \frac{l}{h} \right)^2 \right\}^2. \quad (27)$$

The determinant of the coefficient matrix of  $\Phi_{mn}$  must be equal to 0 in order for the solution of Eq. (22) not to

be  $\Phi_{mn} \equiv 0$ . The shear stress under torsional buckling  $\tau_{cr}$  is determined from this buckling eigen equation, and an exact solution can be obtained with a sufficient number of terms. For example, using the five terms  $\Phi_{11} - \Phi_{33}$ ,  $\tau_{cr}$  is calculated as follows:

$$\tau_{cr} = \frac{9\beta_0\beta_2}{\beta_1\sqrt{\frac{706}{625} + \frac{81}{25}\frac{\beta_2}{\beta_3} + \frac{81}{25}\frac{\beta_2}{\beta_4}}} \sigma_g \tag{28}$$

Timoshenko<sup>(1)</sup> derived the same equations as Eqs. (23)-(28) for the shear buckling stress of plates, except that the above equations add the width  $h$  term for the vertical plates, symmetrically including  $b$  and  $h$  in the shape (interchanging  $b$  and  $h$  results in the same equations). In the equations, if  $h = b$ , then,

$$\tau_{cr} = \frac{9\pi^2}{32} \frac{\left\{1 + \left(\frac{l}{b}\right)^2\right\}^2}{\left(\frac{l}{b}\right)\sqrt{\frac{706}{625} + \frac{81}{25}\left\{\frac{1 + \left(\frac{l}{b}\right)^2}{1 + 9\left(\frac{l}{b}\right)^2}\right\}^2} + \frac{81}{25}\left\{\frac{1 + \left(\frac{l}{b}\right)^2}{9 + \left(\frac{l}{b}\right)^2}\right\}^2}} \sigma_g \tag{29}$$

which matches the equation derived by Timoshenko.

Further, Timoshenko took Eq. (29) to be sufficiently precise for an aspect ratio  $l/b$  (or  $l/h$ ) of 1.5 or lower. This report, however, considers plates that form a beam and assumes that  $l/b$  is 3 or greater, meaning the error will be high when solving for the shear stress under torsional buckling using Eq. (29). If a large number of terms are taken into account, the buckling stress can be determined to a high degree of accuracy even for a  $l/b$  value of 3 or greater; this is impractical, however, as it leads to a complex equation.

### 3.3 Approximation Equation for Shear Buckling Stress

Bearing in mind the conclusions from the previous section, we here propose an approximation equation for determining the shear stress under torsional buckling. The shear buckling stress for a plate of width  $b$  is given by Eq. (10), but  $b$  is included in Euler's buckling stress  $\sigma_e$  and the buckling stress coefficient  $k_s$ . Therefore, the following variables will be defined so that  $b$  and  $h$  can both be considered:

$$\begin{aligned} \hat{\tau}_{bcr} &= \left[ 5.34 + 4.00 \left(\frac{b}{l}\right)^2 \right] \frac{\pi^2 E}{12(1-\mu^2)} \left(\frac{t}{b}\right)^2 \\ &= \left[ 5.34 \left(\frac{l}{b}\right)^2 + 4.00 \right] \frac{\pi^2 E}{12(1-\mu^2)} \left(\frac{t}{l}\right)^2 = \tilde{g}_s \sigma_g \tag{30} \end{aligned}$$

$$\tilde{g}_s = 4.00 + 5.34 \left(\frac{l}{b}\right)^2 \tag{31}$$

where  $\sigma_g$  given by Eq. (21) is a variable independent of  $b$ , and  $\tilde{g}_s$  is the only variable affected by  $b$ . As  $b$  and  $h$  are symmetrically included in the equation to determine the shear stress for torsional buckling described in the previous section, defining  $g_s$  as a revised buckling stress coefficient, replacing  $(l/b)^2$  with  $l/b$  and  $l/h$  for symmetry, and solving for  $g_s$  is sufficient. This is expressed as follows:

$$\tau_{cr} = g_s \sigma_g \tag{32}$$

As the analytical solution for  $g_s$  in the above equation is obtained through the energy method and, as seen from the results of the previous section, is expressed as an infinite series, determining a value for  $g_s$  directly from the analytical solution is not simple. Thus, an equation is derived to approximate  $g_s$  in simplified form. The conditions for the  $g_s$  approximation equation were that it symmetrically include the effects of both horizontal and vertical plates, and that Eqs. (3) and (32) match when  $h = b$ . The following two equations, where  $i$  and  $j$  are integers, are candidate equations that meet the conditions for approximating  $g_s$  in simplified form:

$$\begin{aligned} g_{St} &= 4.00 + 5.34 \frac{\left(\frac{l}{b}\right)^{i+2} + \left(\frac{l}{h}\right)^{i+2}}{\left(\frac{l}{b}\right)^i + \left(\frac{l}{h}\right)^i} \tag{33} \\ g_{Sl} &= 4.00 + 5.34 \frac{\left(\frac{b}{l}\right)^j + \left(\frac{h}{l}\right)^j}{\left(\frac{b}{l}\right)^{j+2} + \left(\frac{h}{l}\right)^{j+2}} \end{aligned}$$

In Sec. 5,  $i$  and  $j$  will be changed to derive a candidate approximation equation. The accuracy of this equation will then be evaluated by comparing to the results of FEM calculations.

#### 4. Buckling Stress Interaction Formula under Combined Stress in Plate Using Energy Method

In this section, we first discuss the buckling stress interaction formulae for plates under various loads, and the similarities between these formulae. Based on these similarities, we then propose an interaction formula relating compressive and shear buckling stresses when an axial compression force and a torsional torque act together upon the box beam. Finally, in Sec. 5, the validity of the proposed formulae is evaluated by comparing them with the results of FEM computations.

##### 4.1 Compressive and Shear Stress

In this section, the buckling stress interaction formula for a compressive stress  $\sigma$  and a shear stress  $\tau$  acting upon a plate is determined based on the energy method. If the out-of-plane displacement due to buckling in Fig. 2 is taken as  $w$ , the out-of-plane displacement  $w$  for a simply supported rectangular plate can be written as:

$$w = \sum_{m=1}^{\infty} \sum_{n=1}^{\infty} C_{mn} \sin \frac{m\pi x}{l} \sin \frac{n\pi y}{b}. \quad (34)$$

The strain energy  $U$ , the work  $W_C$  due to the compressive stress, and the work due to the shear stress  $W_S$  can be expressed as:

$$U = \frac{D}{2} \int_0^b \int_0^l \left[ \left( \frac{\partial^2 w}{\partial x^2} + \frac{\partial^2 w}{\partial y^2} \right)^2 - 2(1-\mu) \left\{ \frac{\partial^2 w}{\partial x^2} \frac{\partial^2 w}{\partial y^2} - \left( \frac{\partial^2 w}{\partial x \partial y} \right)^2 \right\} \right] dx dy, \quad (35)$$

$$W_C = \frac{t}{2} \int_0^b \int_0^l \sigma \left( \frac{\partial w}{\partial x} \right)^2 dx dy, \quad (36)$$

$$W_S = -t \int_0^b \int_0^l \tau \left( \frac{\partial w}{\partial x} \frac{\partial w}{\partial y} \right) dx dy. \quad (37)$$

From these equations, the energy stationary condition is:

$$\frac{\partial}{\partial C_{mn}} (U - W_C - W_S) = 0. \quad (38)$$

The stresses satisfying this condition are expressed as  $\hat{\sigma}'_{cr}$  and  $\hat{\tau}'_{cr}$ , and the buckling stress components when compression and shearing are combined. From the above equations, if only considered when the sum of  $m + n$  is even,<sup>(2)</sup> the same as when a shear stress acts alone, the system of equations for coefficient  $C_{mn}$  is as follows:

$$\frac{\pi^4 D l b}{4} C_{mn} \left[ \left( \frac{m}{l} \right)^2 + \left( \frac{n}{b} \right)^2 \right]^2 - \frac{\hat{\sigma}'_{cr} \pi^2 b t}{4l} m^2 C_{mn} - 8 m n \hat{\tau}'_{cr} t \sum_{i=1}^{\infty} \sum_{j=1}^{\infty} \frac{i j C_{ij}}{(i^2 - m^2)(j^2 - n^2)} = 0. \quad (39)$$

The sums of the above equation are for  $i$  only when  $m + i$  is odd, and for  $j$  only when  $n + j$  is odd. The matrix for the above equation is:

$$\begin{bmatrix} \beta^3 \left( 1 + \frac{1}{\beta^2} \right)^2 - \frac{\beta \hat{\sigma}'_{cr}}{\sigma_e} & -\frac{4}{9} \frac{32 \hat{\tau}'_{cr}}{\pi^2 \sigma_e} & 0 & \dots \\ -\frac{4}{9} \frac{32 \hat{\tau}'_{cr}}{\pi^2 \sigma_e} & 16 \beta^3 \left( 1 + \frac{1}{\beta^2} \right)^2 - \frac{4 \beta \hat{\sigma}'_{cr}}{\sigma_e} & \frac{4}{5} \frac{32 \hat{\tau}'_{cr}}{\pi^2 \sigma_e} & \dots \\ 0 & \frac{4}{5} \frac{32 \hat{\tau}'_{cr}}{\pi^2 \sigma_e} & \beta^3 \left( 1 + \frac{9}{\beta^2} \right)^2 - \frac{\beta \hat{\sigma}'_{cr}}{\sigma_e} & \dots \\ \vdots & \vdots & \vdots & \ddots \end{bmatrix} \begin{Bmatrix} C_{11} \\ C_{22} \\ C_{13} \\ \vdots \end{Bmatrix} = \begin{Bmatrix} 0 \\ 0 \\ 0 \\ \vdots \end{Bmatrix}, \quad (40)$$

$$\beta = \frac{b}{l}. \quad (41)$$

The buckling eigen equation of this coefficient matrix will give an interaction formula, but it has an infinite order. In order to improve the prospects, a buckling eigen equation with low-order terms only ( $C_{11}$  and  $C_{22}$ ) is determined, as shown below:

$$\left[ 1 - \frac{\hat{\sigma}'_{cr}}{\beta^2 \left( 1 + \frac{1}{\beta^2} \right)^2 \sigma_e} \right] \left[ 1 - \frac{\hat{\sigma}'_{cr}}{4 \beta^2 \left( 1 + \frac{1}{\beta^2} \right)^2 \sigma_e} \right] - \left[ \frac{\hat{\tau}'_{cr}}{\frac{9 \pi^2}{32} \beta^3 \left( 1 + \frac{1}{\beta^2} \right)^2 \sigma_e} \right]^2 = 0. \quad (42)$$

The above equation means that the buckling stresses for out-of-plane displacement under buckling, which has an infinite order, can be approximated using only low-order terms as follows:

$$\tilde{\sigma}'_{cr} = \tilde{k}_C \sigma_e, \quad \tilde{k}_C = \beta^2 \left( 1 + \frac{1}{\beta^2} \right)^2, \quad (43)$$

$$\tilde{\tau}_{cr} = \tilde{k}_s \sigma_e, \quad \tilde{k}_s = \frac{9\pi^2}{32} \beta^3 \left(1 + \frac{1}{\beta^2}\right)^2, \quad (44)$$

and the buckling stress interaction formula relating compression and shear can be expressed as follows:

$$\left(1 - \frac{\hat{\sigma}'_{cr}}{\hat{\sigma}_{cr}}\right) \left(1 - \frac{\hat{\sigma}'_{cr}}{4\hat{\sigma}_{cr}}\right) - \left(\frac{\hat{\tau}'_{cr}}{\hat{\tau}_{cr}}\right)^2 = 0, \quad (45)$$

where the superscripted tilde ( $\sim$ ) signifies provisionally approximated values. Thus, for example, if  $\beta = 1$ , the result  $\tilde{k}_c = 4$  matches the exact solution for  $k_c$  (from Eq. (1)), but the result  $\tilde{k}_s = 11.10$  is not accurate when compared to the value of  $k_s = 9.34$  (Eq. (2)) reported by Hayashi.<sup>(2)</sup> As such, in this report, the high-error-margin  $\tilde{\sigma}_{cr}$  and  $\tilde{\tau}_{cr}$  in the above formula are replaced with the exact and highly precise solutions from Eqs. (1) and (3), rewriting the formula as follows:

$$\left(1 - \frac{\hat{\sigma}'_{cr}}{\hat{\sigma}_{cr}}\right) \left(1 - \frac{\hat{\sigma}'_{cr}}{4\hat{\sigma}_{cr}}\right) - \left(\frac{\hat{\tau}'_{cr}}{\hat{\tau}_{cr}}\right)^2 = 0. \quad (46)$$

Thus, for a combined compressive and shear stress, the above formula first uses low-power terms to approximate the infinite series solution for out-of-plane deformation under buckling, then a second-order buckling stress interaction formula is obtained based on the energy method. The resulting formula is thus different from the well-known Eq. (5).

## 4.2 Bending and Shear Stress

Following the approach of the previous section, the buckling stress interaction formula is now determined based on the energy method for the case when a pure bending stress  $\sigma_B$  and shear stress  $\tau$  act upon the plates in Fig. 2. The strain energy of the plate is determined using Eq. (35), the work due to shearing using Eq. (37), and the work  $W_B$  due to the bending stress using the following equation:

$$W_B = \frac{t}{2} \int_0^b \left[ \sigma_B \left(1 - \frac{2}{b}y\right) \int_0^l \left(\frac{\partial w}{\partial x}\right)^2 dx \right] dy. \quad (47)$$

The energy stationary condition is:

$$\frac{\partial}{\partial C_{mn}} (U - W_s - W_B) = 0. \quad (48)$$

From this, the system of equations for coefficient  $C_{mn}$  is as follows:

$$\begin{aligned} & \frac{\pi^2 l b^3}{4} \frac{\pi^2 D}{b^2 t} \left[ \left(\frac{m}{l}\right)^2 + \left(\frac{n}{b}\right)^2 \right]^2 C_{mn} \\ & - 8mn \hat{\tau}'_{cr} \sum_i \sum_j \frac{ij C_{ij}}{(i^2 - m^2)(j^2 - n^2)} \\ & - 4bl \hat{\sigma}'_{Bcr} \left(\frac{m}{l}\right)^2 \sum_j \frac{nj C_{mj}}{(j^2 - n^2)^2} = 0. \end{aligned} \quad (49)$$

The matrix for this system is:

$$\begin{bmatrix} \frac{\pi^2 \beta^3 \sigma_e}{32} \left(1 + \frac{1}{\beta^2}\right)^2 & -\frac{\beta \hat{\sigma}'_{Bcr}}{9} & 0 & \dots \\ -\frac{\beta \hat{\sigma}'_{Bcr}}{9} & \frac{\pi^2 \beta^3 \sigma_e}{32} \left(1 + \frac{4}{\beta^2}\right)^2 & \frac{4\hat{\tau}'_{cr}}{9} & \dots \\ 0 & \frac{4\hat{\tau}'_{cr}}{9} & \frac{\pi^2 \beta^3 \sigma_e}{32} \left(4 + \frac{1}{\beta^2}\right)^2 & \dots \\ \vdots & \vdots & \vdots & \ddots \end{bmatrix} \begin{Bmatrix} C_{11} \\ C_{12} \\ C_{21} \\ \vdots \end{Bmatrix} = \begin{Bmatrix} 0 \\ 0 \\ 0 \\ \vdots \end{Bmatrix}. \quad (50)$$

Further, solving the buckling eigen equation based on using only low-order terms ( $C_{11}$ ,  $C_{12}$ , and  $C_{21}$ ) yields the following:

$$\begin{aligned} & \left[ \frac{\hat{\sigma}'_{Bcr}}{\frac{9\pi^2 \beta^2}{32} \left(1 + \frac{1}{\beta^2}\right) \left(1 + \frac{4}{\beta^2}\right) \sigma_e} \right]^2 \\ & + \left[ \frac{\hat{\tau}'_{cr}}{\frac{9\pi^2 \beta^3}{128} \left(1 + \frac{4}{\beta^2}\right) \left(4 + \frac{1}{\beta^2}\right) \sigma_e} \right]^2 = 1. \end{aligned} \quad (51)$$

As in the previous section, this can be expressed as:

$$\tilde{\sigma}'_{Bcr} = \tilde{k}_B \sigma_e, \quad \tilde{k}_B = \frac{9\pi^2 \beta^2}{32} \left(1 + \frac{1}{\beta^2}\right) \left(1 + \frac{4}{\beta^2}\right), \quad (52)$$

$$\tilde{\tau}'_{cr} = \tilde{k}_s \sigma_e, \quad \tilde{k}_s = \frac{9\pi^2 \beta^3}{128} \left(1 + \frac{4}{\beta^2}\right) \left(4 + \frac{1}{\beta^2}\right). \quad (53)$$

Again,  $\beta = 1$  gives  $\tilde{k}_B = 27.76$  and  $\tilde{k}_s = 17.35$ , which are low-accuracy solutions when compared to the actual values of  $k_B = 23.9$  and  $k_s = 9.34$ . The buckling stress interaction formula Eq. (6) for combined bending and shear stress is solved by replacing with  $\tilde{\sigma}'_{Bcr}$  in Eq. (4) and with  $\tilde{\tau}'_{cr}$  in Eq. (3).

### 4.3 Compressive and Bending Stress

As in Sec. 4. 1, the buckling stress interaction formula for the case when a compressive stress  $\sigma$  and a pure bending stress  $\sigma_b$  act upon the plates in Fig. 2 will be determined based on the energy method. The strain energy is calculated using Eq. (35), the work due to compression using Eq. (36), and the work due to bending using Eq. (47). However, in this section, since the  $x$ -axis displacement can be expressed in the form of a single sine wave,<sup>(2)</sup> the out-of-plane displacement  $w$  is given by:

$$w = \sin \frac{m\pi x}{l} \sum_{n=1}^{\infty} C_n \sin \frac{n\pi y}{b}. \quad (54)$$

Substituting the above equation into Eqs. (35), (36) and (47), the energy stationary condition is:

$$\frac{\partial}{\partial C_n} (U - W_c - W_b) = 0. \quad (55)$$

From this, the following system of equations is obtained for the coefficient  $C_n$ :

$$\begin{aligned} & \frac{\pi^2}{4} \beta^2 \left( m^2 + \frac{n^2}{\beta^2} \right)^2 \sigma_e C_n - \frac{\pi^2}{4} m^2 \hat{\sigma}'_{cr} C_n \\ & - 4 \hat{\sigma}'_{Bcr} m^2 n \sum_j \frac{j}{(j^2 - n^2)^2} C_j = 0, \end{aligned} \quad (56)$$

where the sum for  $j$  is the same as in the previous section. The matrix for this system is:

$$\begin{bmatrix} \frac{\pi^2}{4} \left[ \beta^2 \sigma_e \left( m^2 + \frac{1}{\beta^2} \right)^2 - m^2 \hat{\sigma}'_{cr} \right] & -\frac{8m^2}{9} \hat{\sigma}'_{Bcr} & \dots \\ -\frac{8m^2}{9} \hat{\sigma}'_{Bcr} & \frac{\pi^2}{4} \left[ \beta^2 \left( m^2 + \frac{4}{\beta^2} \right)^2 \sigma_e - m^2 \hat{\sigma}'_{cr} \right] & \dots \\ \vdots & \vdots & \ddots \end{bmatrix} \begin{Bmatrix} C_1 \\ C_2 \\ \vdots \end{Bmatrix} = \begin{Bmatrix} 0 \\ 0 \\ \vdots \end{Bmatrix}. \quad (57)$$

Further, solving the buckling eigen equation based on using only low-order terms ( $C_1$  and  $C_2$ ) yields:

$$\begin{aligned} & \left[ 1 - \frac{\sigma'_{cr}}{\frac{\beta^2}{m^2} \left( m^2 + \frac{1}{\beta^2} \right)^2 \sigma_e} \right] \left[ 1 - \frac{\sigma'_{cr}}{\frac{\beta^2}{m^2} \left( m^2 + \frac{4}{\beta^2} \right)^2 \sigma_e} \right] \\ & - \frac{\sigma'_{Bcr}{}^2}{\left[ \left( \frac{9\pi^2 \beta^2}{32m^2} \right) \left( m^2 + \frac{1}{\beta^2} \right) \left( m^2 + \frac{4}{\beta^2} \right) \sigma_e \right]^2} = 0. \end{aligned} \quad (58)$$

As in the previous section, this can be expressed as:

$$\tilde{\sigma}'_{Bcr} = \tilde{k}_B \sigma_e, \quad \tilde{k}_B = \frac{9\pi^2 \beta^2}{32m^2} \left( m^2 + \frac{1}{\beta^2} \right) \left( m^2 + \frac{4}{\beta^2} \right), \quad (59)$$

$$\tilde{\sigma}'_{cr1} = \frac{\beta^2}{m^2} \left( m^2 + \frac{1}{\beta^2} \right)^2 \sigma_e, \quad \tilde{\sigma}'_{cr2} = \frac{\beta^2}{m^2} \left( m^2 + \frac{4}{\beta^2} \right)^2 \sigma_e. \quad (60)$$

As  $m$  is designed to become the minimum buckling stress, with  $m\beta = 3/2$ , Eq. (59) gives  $\tilde{k}_B = 25.06$ , which differs from the exact solution of  $k_B = 23.9$ . If  $m\beta = 1$  in Eq. (60), the first equation yields:

$$\tilde{\sigma}'_{cr1} = \frac{\beta^2}{m^2} \left( m^2 + \frac{1}{\beta^2} \right)^2 \sigma_e = 4\sigma_e = \hat{\sigma}'_{cr}.$$

This matches the exact solution. Meanwhile, the second equation becomes:

$$\tilde{\sigma}'_{cr2} = \frac{\beta^2}{m^2} \left( m^2 + \frac{4}{\beta^2} \right)^2 \sigma_e = 25\sigma_e = \frac{25}{4} \hat{\sigma}'_{cr}.$$

From the above, using a precise solution for bending when compressive and bending stress act upon a plate yields the following buckling stress interaction formula:

$$\left( 1 - \frac{\hat{\sigma}'_{cr}}{\hat{\sigma}'_{cr}} \right) \left( 1 - \frac{4}{25} \frac{\hat{\sigma}'_{cr}}{\hat{\sigma}'_{cr}} \right) - \left( \frac{\hat{\sigma}'_{Bcr}}{\hat{\sigma}'_{Bcr}} \right)^2 = 0. \quad (61)$$

### 4.4 Similarities between Buckling Stress Interaction Formulae

In Sec. 2 and the previous subsection, the following buckling stress interaction formulae were obtained for a plate acted upon by any two among compressive, shearing, and bending stress:

$$\frac{\hat{\sigma}'_{cr}}{\hat{\sigma}'_{cr}} + \left( \frac{\hat{\tau}'_{cr}}{\hat{\tau}'_{cr}} \right)^2 = 1, \quad (5)$$

$$\left( \frac{\hat{\sigma}'_{Bcr}}{\hat{\sigma}'_{Bcr}} \right)^2 + \left( \frac{\hat{\tau}'_{cr}}{\hat{\tau}'_{cr}} \right)^2 = 1, \quad (6)$$

$$\left( 1 - \frac{\hat{\sigma}'_{cr}}{\hat{\sigma}'_{cr}} \right) \left( 1 - \frac{\hat{\sigma}'_{cr}}{4\hat{\sigma}'_{cr}} \right) - \left( \frac{\hat{\tau}'_{cr}}{\hat{\tau}'_{cr}} \right)^2 = 0, \quad (46)$$

$$\left( 1 - \frac{\hat{\sigma}'_{cr}}{\hat{\sigma}'_{cr}} \right) \left( 1 - \frac{4}{25} \frac{\hat{\sigma}'_{cr}}{\hat{\sigma}'_{cr}} \right) - \left( \frac{\hat{\sigma}'_{Bcr}}{\hat{\sigma}'_{Bcr}} \right)^2 = 0. \quad (61)$$

In this section, we will show the similarities between these equations. Noting the following for clarity,

$$x = \frac{\hat{\sigma}'_{cr}}{\hat{\sigma}_{cr}} \text{ or } \frac{\hat{\sigma}'_{Bcr}}{\hat{\sigma}_{Bcr}}, \quad y = \frac{\hat{\tau}'_{cr}}{\hat{\tau}_{cr}} \text{ or } \frac{\hat{\sigma}'_{Bcr}}{\hat{\sigma}_{Bcr}},$$

the four equations for when two stresses are combined can be written as follows:

$$\begin{aligned} x + y^2 &= 1, \\ (1-x)\left(1 - \frac{1}{4}x\right) - y^2 &= 0, \\ x^2 + y^2 &= 1, \\ (1-x)\left(1 - \frac{4}{25}x\right) - y^2 &= 0. \end{aligned}$$

Viewing these equations from a higher perspective, consider the following equation:

$$(1-x)(1-cx) - y^2 = 0. \tag{62}$$

In Eqs. (5), (6), (46) and (60), the values for  $c$  would be  $c = 0$ ,  $c = -1$ ,  $c = 1/4$  and  $c = 4/25$ , respectively. **Figure 5**<sup>(19)</sup> graphs the change in the formulae with changes in  $c$ . Thus, Eq. (62) indicates that a buckling stress interaction formula for various combined stresses can be collectively represented by introducing a single parameter.

The equations corresponding to  $c = 1/4$ ,  $c = -1$  and  $c = 4/25$  were determined based upon a buckling

eigen equation calculated using the energy method. Meanwhile, since Eq. (5) is an expression of the buckling stress relationship calculated as a regression formula from a theoretical analysis, there is no clear physical meaning for the  $c = 0$  case. However, assuming that there is a suitable  $c$  based on the types of structure and stresses gives meaning to setting  $c$  equal to 0. Also, selecting a suitable  $c$  value should give a buckling stress interaction formula that sufficiently corresponds to the theoretical analysis and FEM calculations.

Approximating the buckling eigen equation obtained with the energy method using low-order terms allows us to determine a buckling stress interaction formula for plates under combined loads. Some of the formulae obtained were the same as well-known formulae, and some differed. Nonetheless, there are demonstrated similarities between the formulae, and they can be related through a single parameter.

Note that the formulae derived in this section assume that buckling deformation can be expressed as a sinusoidal series, including the single-term case. Accordingly, the formulae may not apply if buckling deformation cannot be expressed sinusoidally due to load conditions or boundary conditions. Even in such cases, however, a simplified approximation formula can likely be obtained by changing the  $c$  value.

#### 4.5 Candidate Buckling Stress Interaction Formulae for Compressive and Torsional Stress in Box Beams

In this section, we will discuss the buckling stress interaction formula for the case where an axial compressive force  $P$  and a torsional torque  $T$  act upon a box beam similar to the one in Fig. 1. Equation (5) is a known buckling stress interaction formula for the case where shearing and compression act upon a rectangular plate. Also, Eq. (46) based on the energy method was proposed in Sec. 4.3.

As in Sec. 4.1, an approximate buckling stress interaction formula for  $P$  and  $T$  acting upon a box beam can be determined with the energy method, but it is cumbersome to use due to there being four plates. Still, since compressive and shear stresses are acting upon the four plates comprising the beam section, a relationship similar to that for plates is expected. Thus, Eqs. (63) and (64) are proposed as candidate buckling stress interaction formulae for box beams.

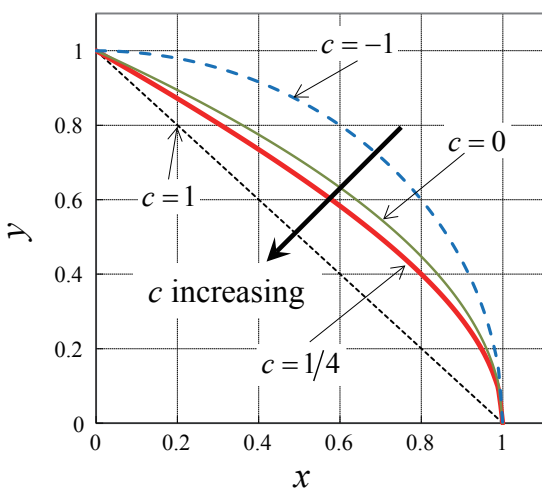


**Fig. 5** Variation of buckling stress interaction formula with parameter  $c$ .

These formulae take  $\sigma_{cr}$  as the compressive buckling stress for box beams as calculated by Kuranishi<sup>(13-16)</sup> (Fig. 3) and  $\tau_{cr}$  as the shear buckling stress introduced in Sec. 3, as well as  $\sigma'_{cr}$  and  $\tau'_{cr}$  as the compressive and shear buckling stress components for combined axial compression and torsion. The accuracy of the formulae will be evaluated by comparing to the results of FEM calculations in Sec. 5.

$$\frac{\sigma'_{cr}}{\sigma_{cr}} + \left(\frac{\tau'_{cr}}{\tau_{cr}}\right)^2 = 1 \quad (63)$$

$$\left(1 - \frac{\sigma'_{cr}}{\sigma_{cr}}\right) \left(1 - \frac{\sigma'_{cr}}{4\sigma_{cr}}\right) - \left(\frac{\tau'_{cr}}{\tau_{cr}}\right)^2 = 0 \quad (64)$$

### 5. Validation Using Finite Element Method

In this section, the accuracy of the shear buckling stress approximation equations introduced in Sec. 3 and the buckling stress interaction formulae introduced in Sec. 4 is evaluated by comparison with FEM computations results.

#### 5.1 Computation Model and Conditions

In order to verify the equations introduced in Secs. 3 and 4, FEM computations were performed for the box beam in Fig. 1 with width  $b$ , height  $h$ , length  $l$ , and thickness  $t$ . **Figure 6**<sup>(20)</sup> shows the FEM mesh created using generic analysis code in ANSYS as the FEM solver. The element size is 2.5 mm for both length and width, and 4-node shell elements (SHELL 181) were used. The loading point is the center

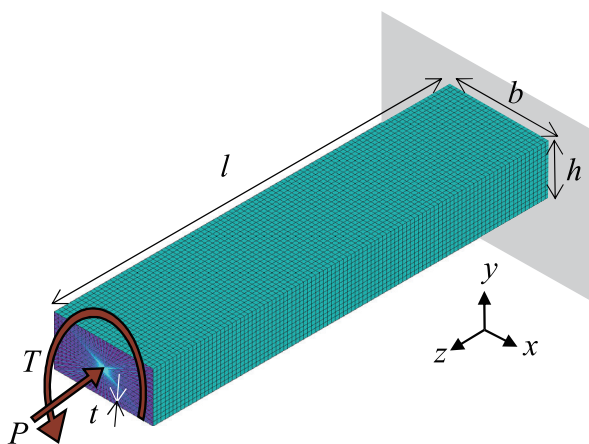


**Fig. 6** Outline of finite element model for box beam.

of one end of the section, with rigid bars connecting the center point and all nodes on the end surface. The translational degrees of freedom for all nodes on the opposite end are constrained.

In order to verify the accuracy of Eqs. (32) and (33) relating the approximation equations for shear buckling stress, buckling eigenvalues were analyzed for the specifications given in **Table 1**.

For a combined compressive force  $P$  and torsional torque  $T$ , the ratio of  $P$  to  $T$  is varied as shown in **Table 2** to perform an buckling eigenvalue analysis. The ratio of the compressive stress  $\sigma$  and shear stress  $\tau$  when  $P$  and  $T$  act on the plate is calculated as given below, using the parameter  $\zeta$ :

$$\sigma : \tau = (1 - \zeta) : \zeta = \frac{P}{2(b+h)t} : \frac{T}{2bht}, \quad (65)$$

where  $\zeta = 0$  when the load is pure compression and  $\zeta = 1$  when the load is pure torsion (pure shearing).

**Table 1** Dimensions of finite element model for box beam [mm].

Label	Length ( $l$ )	Width ( $b$ )	Height ( $h$ )	Thickness ( $t$ )
S1	300	80	20, 25, 30, 35, 40, 45, 50	0.8
S2	300	90	30, 35, 40, 45, 50, 60, 80, 90	1.0
S3	400	80	30, 40, 50, 70	1.0
S4	400	90	25, 35, 40, 45, 50	1.0
S5	400	100	25, 30, 40, 50, 60, 70, 80, 90, 100	1.0
S6	500	120	30, 35, 40, 50, 60, 70, 80	1.2

**Table 2** Dimensions of finite element model for box beam for compression and torsion [mm].

Label	Length ( $l$ )	Width ( $b$ )	Height ( $h$ )	Thickness ( $t$ )
C1	300	90	40	1.0
C2	300	90	60	1.0
C3	300	90	80	1.0
C4	400	100	50	1.0
C5	400	100	60	1.0
C6	400	100	80	1.0
C7	400	100	100	1.0
C8	500	120	50	1.2
C9	500	120	110	1.2

### 5.2 FEM Verification of Buckling Stress for Box Beam under Torsion

Figure 7<sup>(20)</sup> shows the results of an example buckling mode for buckling eigenvalue analysis. The shear buckling stress is plotted as a function of the sectional aspect ratio ( $\delta = h/b$ ) in Fig. 8.<sup>(20)</sup> The labels correspond to those listed in Table 1. The stress errors in Fig. 9<sup>(20)</sup> are determined by comparing values calculated using candidate equations with  $i = 1$  and  $j = 0, 1$  and  $2$  based on Eq. (33) for the shear buckling stress under torsion with the results of FEM computations by the following equation, with  $\tau_{crFEM}$  being the FEM-computed shear force and  $\tau_{crCurrent}$  being the shear force calculated from the candidate equation:

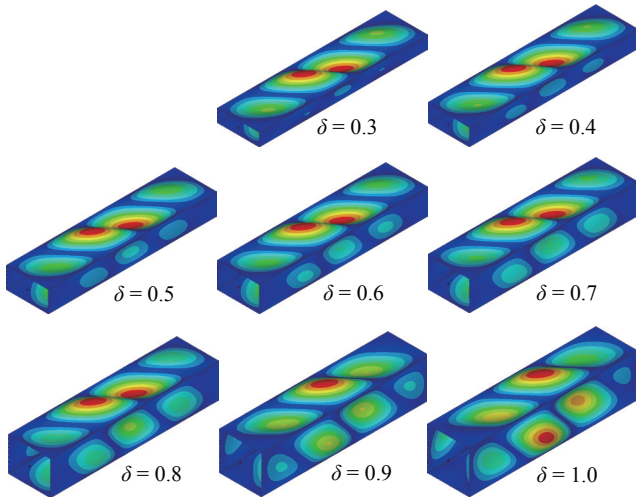


Fig. 7 FEM results for buckling mode under torsion (S5  $l = 400, b = 100, h = 30-100, t = 1.0$  mm).

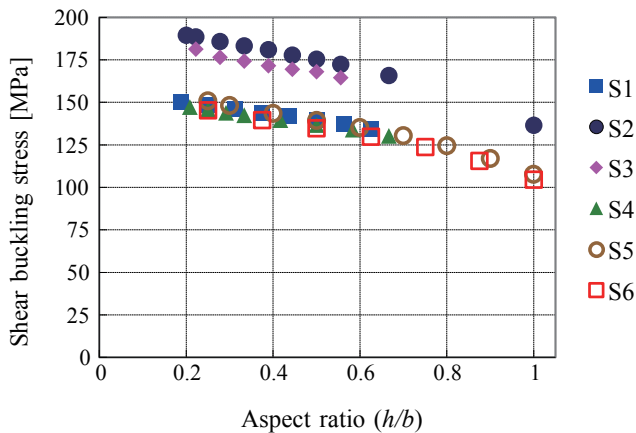


Fig. 8 FEM results for dependence of torsional buckling stress on aspect ratio of cross section.

$$\text{Error} [\%] = \frac{\tau_{crCurrent} - \tau_{crFEM}}{\tau_{crFEM}} \times 100 . \tag{66}$$

The values calculated using Eq. (33) exceed the FEM values more as  $i$  increases. They are larger than the FEM values for  $j = 0$ , but lower than the FEM values for  $j \geq 2$ . Thus, the smallest error is obtained for  $j = 1$ , yielding the following equation:

$$g_s = 4.00 + 5.34 \frac{\frac{b}{l} + \frac{h}{l}}{\left(\frac{b}{l}\right)^3 + \left(\frac{h}{l}\right)^3} . \tag{67}$$

The error calculated using the above equation is shown in Fig. 10.<sup>(20)</sup> Within the practical aspect ratio range ( $h/b \geq 0.4$ ), the error is less than about 5%. Figure 11<sup>(20)</sup> compares the buckling stress calculated using Eq. (67) with the FEM results for specification S5.

### 5.3 FEM Verification of Buckling Stress Interaction Formula for Compressive and Torsional Stress

FEM results for the buckling mode for a beam with  $l = 400, b = 100, h = 50$  and  $t = 1.0$  mm are shown in Fig. 12,<sup>(20)</sup> and the buckling stress in Eq. (65) is shown in Fig. 13<sup>(19)</sup> versus the parameter  $\zeta$ . Figure 14<sup>(20)</sup> compares curves produced using Eqs. (63) and (64) with the stress ratios computed by the FEM. It can be seen that Eq. (63) produces results that are closer to the FEM computations. Figure 15<sup>(20)</sup> plots the difference between the results produced by Eq. (63) and the FEM computations, expressed as:

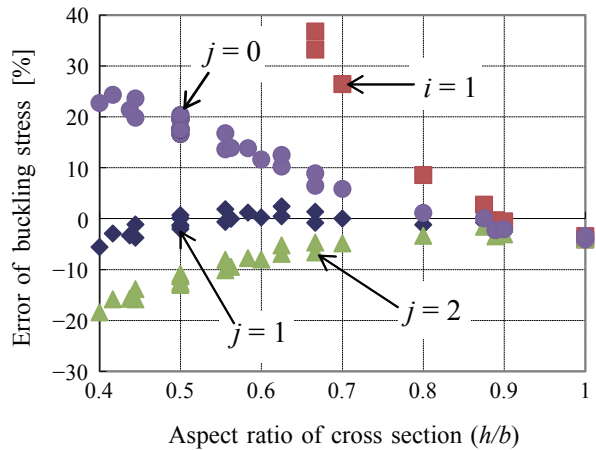


Fig. 9 Shear buckling stress error vs. aspect ratio of cross section.

$$\text{Diff}[\%] = \left[ \frac{\sigma'_{crFEM}}{\sigma_{crFEM}} + \left( \frac{\tau'_{crFEM}}{\tau_{crFEM}} \right)^2 - 1 \right] \times 100, \quad (68)$$

where  $\sigma_{crFEM}$  and  $\tau_{crFEM}$  represent the FEM computed compressive and torsional buckling stresses, respectively, and  $\sigma'_{crFEM}$  and  $\tau'_{crFEM}$  are the buckling stress components computed from the FEM buckling eigenvalue analysis for combined compressive and torsional stress. The labels correspond to those listed in Table 1. It can be seen that the largest differences appear at about  $\zeta = 0.4$ . This is the effect of the aspect ratio  $\delta$  of the beam section. As  $\delta$  approaches 1 and the section becomes more square, greater deviation occurs between the two sets of results. Given that this

deviation is as large as 12%, the accuracy of Eq. (63) is not very high.

As described in Sec. 4. 4, the compressive and shear buckling stress interaction formulae Eqs. (63) and (64) can be expressed as the formula below, using the parameter  $c$ .

$$\left( 1 - \frac{\sigma'_{cr}}{\sigma_{cr}} \right) \left( 1 - c \frac{\sigma'_{cr}}{\sigma_{cr}} \right) - \left( \frac{\tau'_{cr}}{\tau_{cr}} \right)^2 = 0 \quad (69)$$

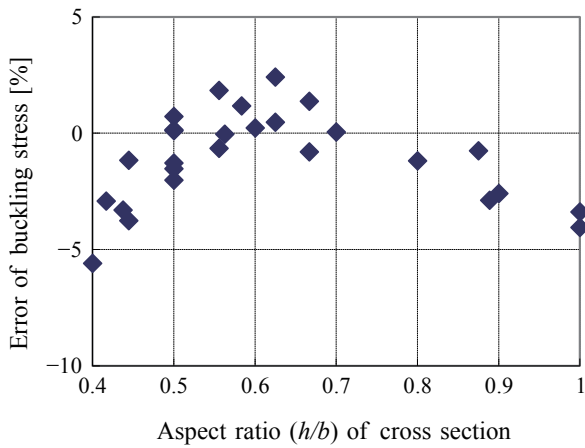


**Fig. 10** Dependence of error in shear buckling stress obtained using Eq. (67) on aspect ratio of cross section.

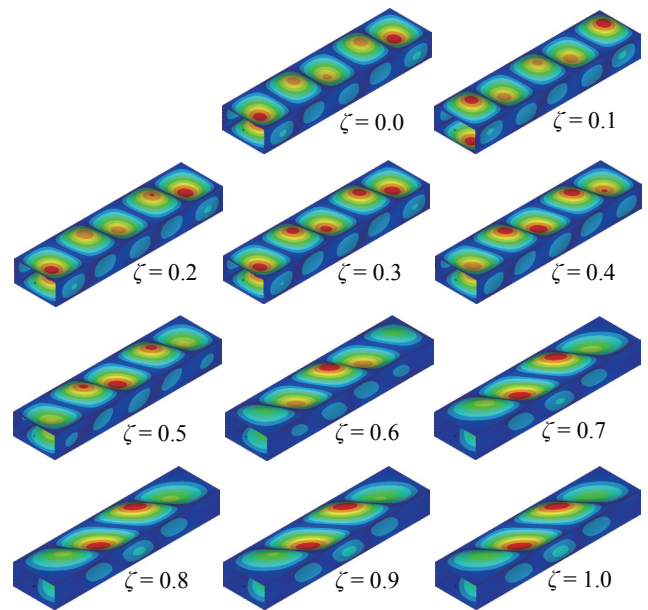


**Fig. 12** Buckling modes determined by FEM ( $l = 400$ ,  $b = 100$ ,  $h = 50$ ,  $t = 1.0$  mm,  $\zeta = 0.0-1.0$ ).

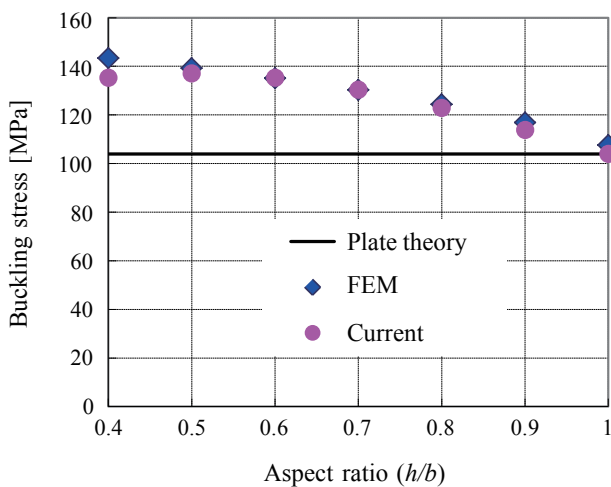


**Fig. 11** Comparison of buckling stress obtained by FEM, plate theory, and current method (S5  $l = 400$ ,  $b = 100$ ,  $h = 40-100$ ,  $t = 1.0$  mm).

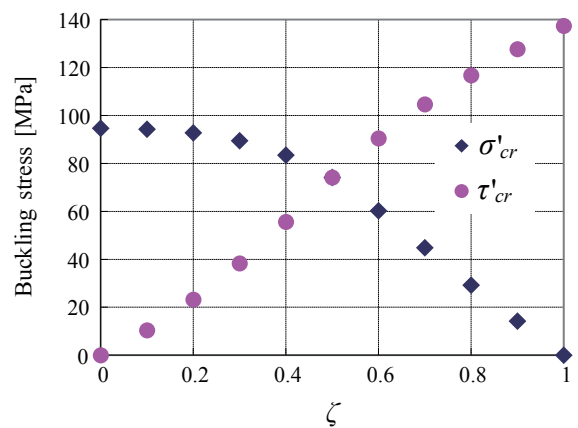


**Fig. 13** Dependence of buckling stress on stress ratio as determined by FEM (C3  $l = 400$ ,  $b = 100$ ,  $h = 50$ ,  $t = 1.0$  mm,  $\zeta = 0.0-1.0$ ).

By setting  $c = -1/4$  (or  $c = -0.249$ , if calculated using the least squares method), for example, a formula with sufficient accuracy can be obtained for compressive and torsional buckling for the box beam (Fig. 16).<sup>(20)</sup>

As described in Sec. 4, Eq. (64) was derived by assuming that buckling deformation could be expressed as a sinusoidal series. However, Wittrick and Curzon<sup>(17,18)</sup> assumed that buckling distortion included both sine waves and hyperbolic functions and derived a buckling stress interaction formula for compressive and torsional stress in infinitely long rectangular plates. As shown in Fig. 4, this formula for beams is different to that for compressive and shear stresses in plates, and the buckling deformation mode is different

when the stress ratio  $\zeta$  is less than or greater than about 0.38. Thus, the range  $0 \leq \zeta \leq 1$  cannot be described using a single formula. The result by Wittrick and Curzon, the curve from Eq. (69) for  $c = -1/4$ , and some FEM results ( $l = 400, b = 100, t = 1.0, h = 50$  ( $\delta = 0.5, C4$ ),  $100$  ( $\delta = 1, C7$ ) mm) are compared in Fig. 17.<sup>(20)</sup> It can be seen that the beam section results approach the curve by Wittrick and Curzon as the aspect ratio  $\delta$  approaches 1, and the curve approaches  $c = -1/4$  as it flattens out.

However, the buckling deformation mode could differ due to differences in the structure or loading conditions, making it unclear what kind of  $c$  value is appropriate and what structural parameters affect  $c$ .

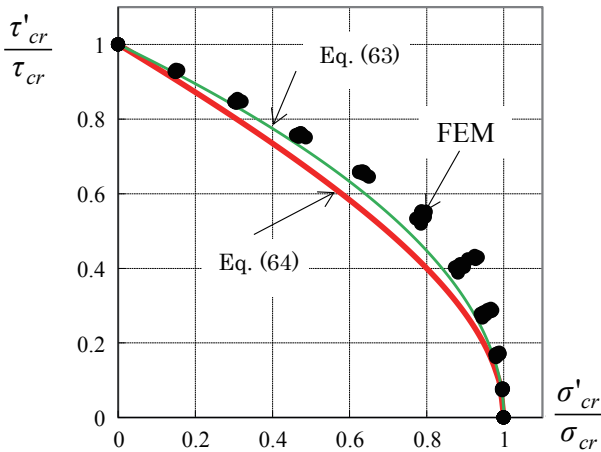


Fig. 14 Comparison of buckling stress interaction formulae and FEM results.

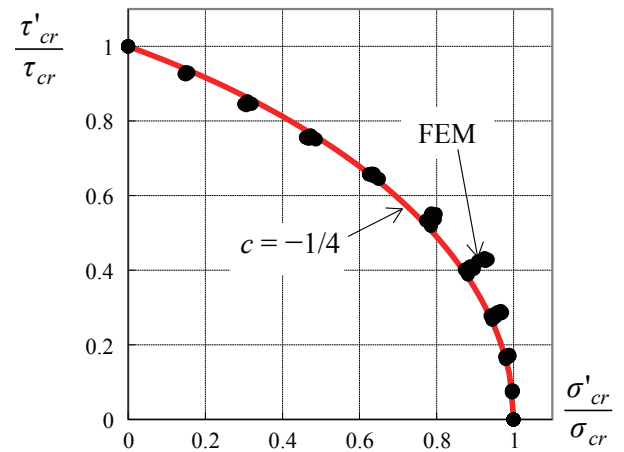


Fig. 16 Comparison of buckling stress interaction formula with  $c = -1/4$  with FEM results.

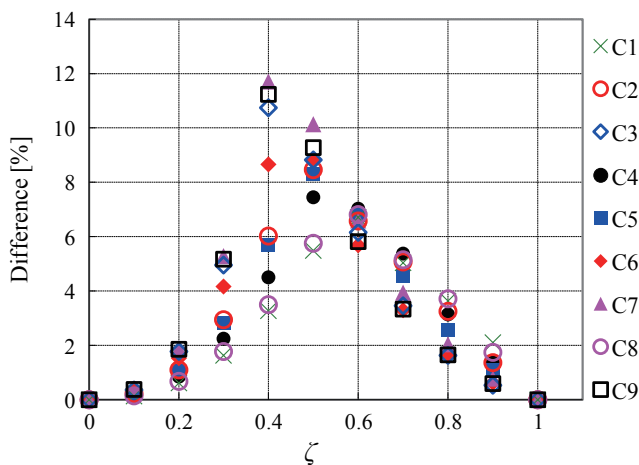


Fig. 15 Difference in stress ratio determined using Eq. (63) and FEM results.

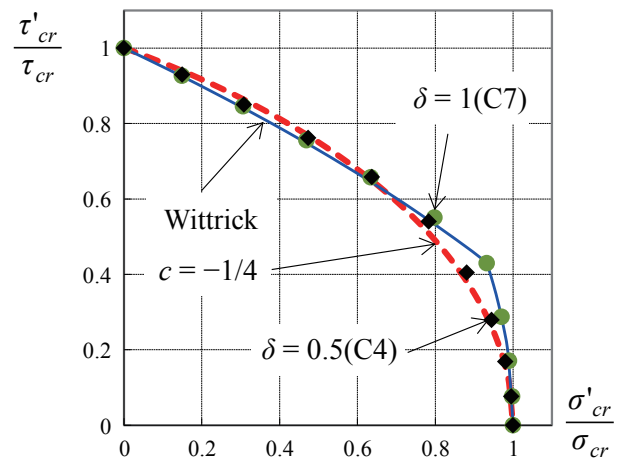


Fig. 17 Comparison of buckling stress interaction formula with  $c = -1/4$  and curve published by Wittrick and Curzon<sup>(17)</sup> with FEM results ( $l = 400, b = 100, t = 1.0, h = 50$  ( $\delta = 0.5, C4$ ),  $100$  ( $\delta = 1, C7$ ) mm).

## 6. Conclusion

This report began by discussing simplified methods for determining the shear buckling stress under torsion for box beams. An equation for approximating the shear buckling stress was proposed, and was verified for accuracy against the results of a buckling eigenvalue analysis using FEM. Next, buckling stress interaction formulae were introduced for a combination of an axial compressive force and a torsional torque on a thin-walled box beam. First, a buckling stress interaction formulae was derived based on the energy method for a single plate. Based on this result, an interaction formula for compressive and torsional buckling stress was proposed, and its accuracy was verified by comparing to the results of an FEM buckling eigenvalue analysis. The conclusions were as follows:

(1) Based on a buckling eigen equation derived using the energy method, the conventional shear buckling stress equation and buckling stress coefficient were rewritten to enable simultaneous and symmetrical treatment of widths for both horizontal and vertical plates in order to propose an approximation equation for determining the shear stress under torsional buckling in a box beam. Based on a comparison with the FEM results, the proposed approximation equation was found to exhibit an error of less than about 5% for sectional aspect ratios of 0.4-1.0, which is an acceptable level of accuracy.

(2) Assuming that the buckling mode was sinusoidal, approximating the buckling eigen equation obtained with the energy method using low-order terms allowed us to derive a buckling stress interaction formula for plates under combined loads. There were demonstrated similarities between the formulae obtained, and they could be related through a single parameter. The proposed formulae for compressive and torsional buckling stress in box beams were found to differ depending upon the load ratio and sectional aspect ratio.

## Acknowledgement

Valuable outcome in this report is the results obtained by the joint research with Toyota Motor Corporation. We express respectful gratitude to Mr. Tsutomu Hamabe, Mr. Norihisa Aoki and Mr. Hideo Takeda of Toyota Motor Corporation in

relation to a patient joint research over the years in spite of slow progress.

## References

- (1) Timoshenko, S. P., *Theory of Elastic Stability*, 2nd Ed. (1961), 541p., McGraw-Hill.
- (2) Hayashi, T., *Keikouzou no Riron to sono Ouyou (Jou)* (in Japanese) (1966), 194p., *Nihon Kagaku Gijutsu Renmei*.
- (3) Column Research Committee of Japan, *Handbook of Structural Stability* (1971), 1048p., Corona Pub. Co.
- (4) Ziemian, R. D., *Guide to Stability Design Criteria for Metal Structures*, 6th Ed. (2010), pp. 128-145, John Wiley & Sons, Inc.
- (5) Kobayashi, S., *Koukuuki Kouzou Rikigaku, Zouhoshinpan* (in Japanese) (2014), pp. 141-148, Pleiades Pub. Co.
- (6) Sakai, T., "On the Relation between Energy and Galerkin's Methods for Problems of Mechanics", *Bull. Fac. Eng., Hokkaido University* (in Japanese), Vol. 1S (1948), pp. 167-185.
- (7) Akasaka, T. and Yoshida, H., *Zairyo oyobi Kozo Gijutsusha no tameno Jitsuyo Enerugiho* (in Japanese) (2000), 273p., *Youkendou*.
- (8) von Karman, T., Sechler, E. E. and Donnell, L. H., "The Strength of Thin Plates in Compression", *Trans. ASME*, Vol. 54 (1932), pp. 53-56.
- (9) Yu, W.-W., *Cold-formed Steel Design*, 3rd Ed. (2000), 756p., John Wiley & Sons, Inc.
- (10) AISI/CARS 2002, GAS (Geometric Analysis of Sections) (2002), American Iron and Steel Institute & Auto/Steel Partnership, (CD-ROM).
- (11) Kobayashi, S. and Kondou, K., *Dansei Rikigaku* (in Japanese) (1987), 305p., *Baifuukan*.
- (12) Byon, O. and Uemura, M., "Post-buckling Behaviors of Flat Plates under Axial Compression, 1st Rep., Discussion of Secondary Buckling Values by Analytical Method", *Rep. Aeronaut. Res. Inst. Univ. Tokyo* (in Japanese), Vol. 12, No. 2 (1976), pp. 477-496.
- (13) Kuranishi, M., "Several Kinds of Elastic Instability of Thin Plane-walled Struts under Axial Compressive Load, and Condition of Minimum Weight", *J. Soc. Naval Architects* (in Japanese), Vol. 1935, No. 56 (1935), pp. 127-143.
- (14) Kuranishi, M., "The Wall Buckling Strength of Thin Plane Walled Struts under Axial Compressive Load, 1st Report", *J. Jpn. Soc. Aeronaut. Eng.* (in Japanese), Vol. 2, No. 3 (1935), pp. 55-86.
- (15) Kuranishi, M., "The Wall Buckling Strength of Thin Plane Walled Struts under Axial Compressive Load, 2nd Report", *J. Jpn. Soc. Aeronaut. Eng.* (in Japanese), Vol. 2, No. 4 (1935), pp. 259-284.
- (16) Kuranishi, M., "The Wall Buckling Strength of Thin Plane Walled Struts under Axial Compressive Load, 3rd Report", *J. Jpn. Soc. Aeronaut. Eng.* (in Japanese), Vol. 2, No. 5 (1935), pp. 485-508.

- (17) Wittrick, W. H. and Curzon, P. L. V., "Stability Functions for the Local Buckling of Thin-walled Structures in Bending and Compression", *Aeronaut. Quarterly* (1968), pp. 327-351.
- (18) Wittrick, W. H. and Curzon, P. L. V., "Local Buckling of Long Polygonal Tubes in Combined Compression and Torsion", *Int. J. Mech. Sci.*, Vol. 10 (1968), pp. 849-857.
- (19) Furuu, K., Amago, T., Nakagawa, T., Hamabe, T. and Aoki, N., "Buckling Stress Relation Equations of Box Beam under Compression and Torsion", *Trans. JSME* (in Japanese), Vol. 80, No. 816 (2014), DOI : 10.1299/transjsme.2014smm0219.
- (20) Furuu, K., "Studies on the Buckling of the Box Beam Composed of Thin Plates", *Dr. Thesis, Seikei University* (in Japanese) (2015), 122p.
- (21) Iguchi, S., "Die Knickung der Rechteckigen Platte durch Schubkrafte", *Ingenieur-archiv*, Vol. 9 (1938), pp. 1-12.
- (22) Iguchi, S., "Die Knickung der Vierseitig Eingespannten Rechteckigen Platte durch Schubkrafte", *Proc. Physico-mathematical Soc. Jpn.*, 3rd, Vol. 20 (1938), pp. 814-832.
- (23) Chwalla, E., "Beitrag zur Stabilitatstheorie des Stegbleches Vollwandiger Trager", *Der Stahlbau*, Vol. 9 (1936), pp. 161-166.
- (24) Johnson, Jr. A. E. and Buchert, K. P., "Critical Combinations of Bending, Shear, and Transverse Compressive Stresses for Bucking of Infinitely Long Flat Plates", *NACA Technical Note*, No. 2536 (1951).

Figs. 1, 5 and 13

Reprinted from *Trans. JSME* (in Japanese), Vol. 80, No. 816 (2014), Furuu, K., Amago, T., Nakagawa, T., Hamabe, T. and Aoki, N., Buckling Stress Relation Equations of Box Beam under Compression and Torsion, © 2014 The Japan Society of Mechanical Engineers.

---

### Katsuya Furuu

Research Field:

- Structural Analysis

Academic Degree: Dr.Eng.

Academic Societies:

- The Japan Society of Mechanical Engineers

- Society of Automotive Engineers of Japan




---

### Tatsuyuki Amago

Research Fields:

- Design by the Structural Analysis

- Spot Welding

Academic Societies:

- The Japan Society of Mechanical Engineers

- Society of Automotive Engineers of Japan

- Japan Welding Society




---

### Toshiaki Nakagawa

Research Fields:

- Mass Management

- Noise and Vibration

Academic Degree: Dr.Eng.

Academic Societies:

- The Japan Society of Mechanical Engineers

- Society of Automotive Engineers of Japan

